Provided for non-commercial research and education use.
Not for reproduction, distribution or commercial use.

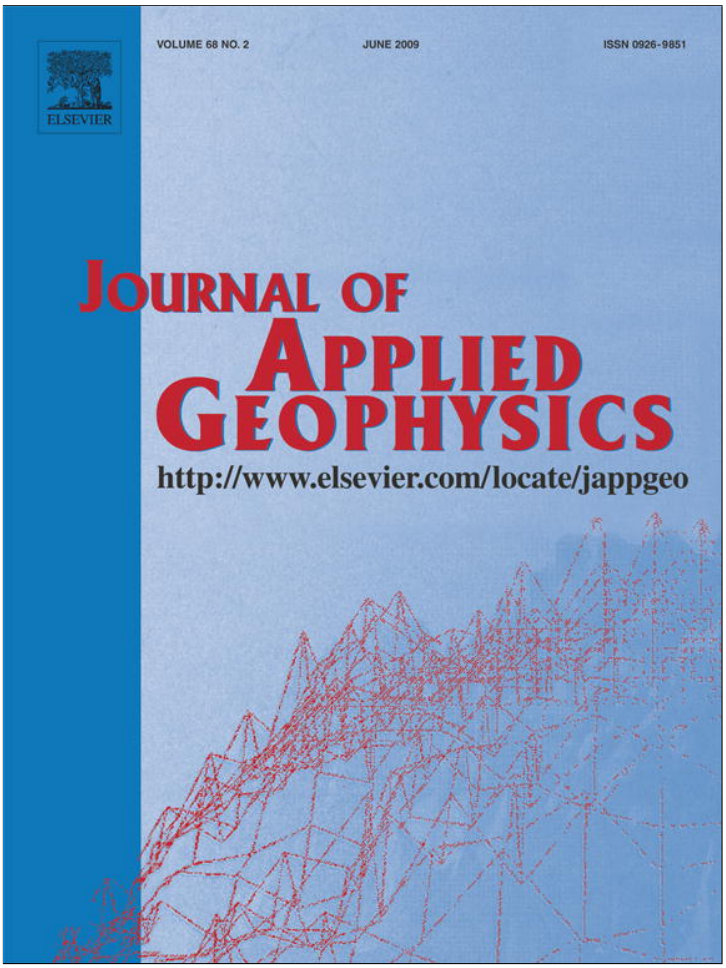

This article appeared in a journal published by Elsevier. The attached copy is furnished to the author for internal non-commercial research and education use, including for instruction at the authors institution and sharing with colleagues.

Other uses, including reproduction and distribution, or selling or licensing copies, or posting to personal, institutional or third party websites are prohibited.

In most cases authors are permitted to post their version of the article (e.g. in Word or Tex form) to their personal website or institutional repository. Authors requiring further information regarding Elsevier's archiving and manuscript policies are encouraged to visit:

http://www.elsevier.com/copyright

Author's personal copy

Journal of Applied Geophysics 68 (2009) 294–300

Contents lists available at ScienceDirect

Journal of Applied Geophysics

journal homepage: www.elsevier.com/locate/jappgeo

Comparison between electromagnetic induction and fluxgate gradiometer measurements on the buried remains of a 17th century castle

David Simpson [a,*], Alexander Lehouck [b], Lieven Verdonck [c], Hans Vermeersch [a], Marc Van Meirvenne [a], Jean Bourgeois [c], Erik Thoen [b], Roald Docter [c]

[a] Department of Soil Management, Ghent University, Coupure 653, B-9000 Gent, Belgium
[b] Department of Medieval History, Ghent University, Blandijnberg 2, B-9000 Gent, Belgium
[c] Department of Archaeology and Ancient History of Europe, Ghent University, Blandijnberg 2, B-9000 Gent, Belgium

ARTICLE INFO

Article history:
Received 18 February 2008
Accepted 16 March 2009

Keywords:
Archaeological prospection
Coil orientation
Electromagnetic induction
In-phase response
Magnetic susceptibility
Electrical conductivity

ABSTRACT

This study aimed to evaluate the different configurations of an electromagnetic induction (EMI) sensor, the EM38DD (Geonics Limited, Canada) with fluxgate gradiometer measurements on an archaeological site. The EM38DD allows measuring both the apparent magnetic susceptibility (MSa or χ_a) and the apparent electrical conductivity (ECa or σ_a) in two different coil orientations. A gradiometer measures the lateral variations of the vertical magnetic field gradient, caused by the induced and remanent magnetisations. An archaeological site where historical documents indicated the presence of a 17th century brick castle was selected as a test area. The results of the first survey with the EM38DD showed very strong magnetic anomalies in the central field, which were caused by the brick remains of the castle. Therefore, a smaller area was chosen within this field to compare the different configurations of the EM38DD with the gradiometer at the same measurement resolution. The most useful results with the EM38DD were obtained from the MSa measured in a vertical coplanar orientation. Its anomalies corresponded well with the gradiometer anomalies. The gradiometer anomalies were sharper defined than the EM38DD anomalies, but were complicated by the bipolar response pattern. The MSa map in horizontal coplanar orientation was very difficult to interpret, due to the less optimal spatial sensitivity. The wall remains were not visible in the ECa map in horizontal coplanar orientation, although other interesting anomalies were detected.
© 2009 Elsevier B.V. All rights reserved.

1. Introduction

Anomalies of magnetic properties are a useful indicator of human disturbance in soil. For this reason, gradiometers are routinely used in archaeological prospection (Gaffney and Gater, 2003). Gradiometers measure passively small deviations from the earth's magnetic field, as remanent magnetism from past magnetisations as well as present magnetic induction of magnetic susceptible materials.

Electromagnetic induction (EMI) is less frequently used, but also allows measuring the apparent magnetic susceptibility (MSa or χ_a), whereby a magnetic field is artificially generated. So, in theory, sensors based on EMI are able to measure similar anomalies due to magnetic susceptible materials as gradiometers. In practice however, EMI is far less often used to measure magnetic susceptibility than gradiometers (e.g. English Heritage, 1995). Tabbagh (1984) compared magnetic and electromagnetic prospection to detect magnetic anomalies with theoretical models. He found differences in the modelled spatial response to magnetic features due to the different nature of the magnetising field. Gradiometer measurements were more influenced by metal objects, creating a larger area so that subtle anomalies were masked by extreme values. On the other hand, Desvignes and Tabbagh (1995) tested their EMI prototype and a Caesium gradiometer on a brick workshop site and a neolithic ring ditch site, which resulted in very similar anomaly maps. Persson and Olofsson (2004) used both the electrical conductivity (ECa or σ_a) and the MSa, which corresponded in different degrees to both GPR (ground penetrating radar) and gradiometer maps.

However, other case studies do not always show a good resemblance between the gradiometer and EMI sensor data, because the evaluation of EMI instruments for archaeological prospection is often done without considering the MSa, as in Fröhlich et al. (1996) and Maillol et al. (2004). Linford (1998) compared both the ECa and MSa of an EM38 instrument with twin probe resistivity and fluxgate gradiometer data. The ECa showed more resemblance to the gradiometer than to the resistivity map but his test area was very low in ECa, so that the signal was probably masked by the small influence of the magnetic susceptibility in the ECa measurement (Tabbagh, 1990). One of the reasons of changing success with an EMI sensor is the diversity of measurement configurations that can be used. Both MSa and ECa can be measured in different coil orientations and coil distances, each having a distinct spatial sensitivity.

A disadvantage of an EMI sensor like the EM38 is that it can only measure one property (either ECa or MSa) at a time. Therefore at least two surveys are needed to measure both, duplicating the total survey time. And then the measurements are also not collocated and not

* Corresponding author.
E-mail address: David.Simpson@UGent.be (D. Simpson).

0926-9851/$ – see front matter © 2009 Elsevier B.V. All rights reserved.
doi:10.1016/j.jappgeo.2009.03.006

Author's personal copy

taken under identical ambient conditions. So investigating their relationship involves interpolation uncertainty. Contrarily, the EM38DD sensor (Geonics Limited, Canada) is able to measure ECa in both the vertical and the horizontal coplanar orientations (Cockx et al., 2007). The EM38DD is also able to measure simultaneously ECa and MSa (Simpson et al., 2008). Such collocated observations have a much better potential to investigate their relationship and complementarity than a single EMI instrument. But so far there has not been a systematic evaluation of the different options the EM38DD offers.

The objective of this study was to evaluate the different EM38DD configurations, installed on a mobile platform guided by a dGPS, for archaeological prospection. The significant advantage of this system is the fast acquisition of simultaneous and colocated ECa and MSa measurements. These measurements were compared with a fluxgate gradiometer survey. An archaeological site containing the buried remains of a 17th century castle was selected as a test case.

2. Materials and methods

2.1. Study site

The study site was located in Vinkem, a small village near the west coast of Belgium (51°00′50.2292″ N, 2°39′40.8037″ E) (Fig. 1). The site consisted of three pasture fields of 0.8, 0.8 and 0.5 ha. The central field was surrounded by a large ditch of approximately 5 m wide. The site was located on a plateau of Tertiary clay, close to the edge of the low coastal area, 8.5 m above the mean sea level (expressed in m TAW, "Tweede Algemene Waterpassing", the reference level of the Belgian ordnance). The regional topography was flat to slightly undulating. The tertiary clay was covered by a shallow aeolian deposit, consisting of loam (Soil Taxonomy) from the Weichselian Lateglacial. The deeper sediments (from earlier Weichselian periods) were more silty than the upper sediments and they contain free $CaCO_3$ (T'Jonck and Moormann, 1962). The average depth of the groundwater was about 1 m, with a moderately wet soil moisture status throughout most of the year.

2.2. Historical background

The history of the site was investigated by Lehouck et al. (2007). Vinkem was a prosperous village during the early 16th century until religious wars (known as the Eighty Years War) disturbed the region in the second half of the 16th century. The outcome of this instable period was a large-scale depopulation of the agrarian communities, resulting in abandoned and destroyed holdings and farms. Around 1600, stability had returned to the region, attracting wealthy nobles to purchase the undervalued land (today still considered as very fertile) and initiating an increased building activity. The origin of the castle at the study site dated back to this period of the early 17th century. It was erected by the lords "de Moucheron". A military map made by count de Ferraris at the end of the 18th century (Fig. 2a) clearly showed the presence of buildings at the site, surrounded by a large ditch and an entrance in the south. The cadastral map of circa 1820 (Fig. 2b) showed the same site, with a very accurate delineation of the castle, surrounding buildings, a gate at the southern entrance and an entrance bridge over the ditch in the east. Although both maps indicated the presence of several buildings, they have been made for different purposes and therefore had a different spatial accuracy. The distribution of the site in various cadastral units suggested that the castle was partially leased out and used as a second residence, which was probably the case during the second half of the 18th century when the lords transposed their residence to the city. Similar examples can be shown in Flanders from the end of the 17th century on Lambrecht (2002).

By the middle of the 19th century the castle was left to decay and eventually demolished in 1876. The remains of the castle were largely reused as building material. From this period on the site was exploited as a pasture land. No image was available of the castle. The only representative idea of the castle could be derived from contemporary buildings in the region. In view of exhibiting the site to the public, the question was what remained of the buildings and where the remains were located.

2.3. Geophysical measurements

The EM38DD is a frequency domain EMI sensor of the "slingram" type. This sensor consists of two single EM38 sensors that are attached perpendicularly to each other. To avoid interference, one of the paired instruments of the EM38DD works at a slightly different frequency. Each sensor has two coils separated by 1 m, where one acts as the transmitter and the other as the receiver coil. The perpendicular arrangement results in two coil orientations: horizontal and vertical coplanar. An alternating current is passed through the transmitter coil that generates a primary electromagnetic field. This primary field induces eddy currents in the soil, which on their turn generate a secondary electromagnetic field. The strength of the eddy currents and consequently of the secondary field (in quadrature-phase (QP)

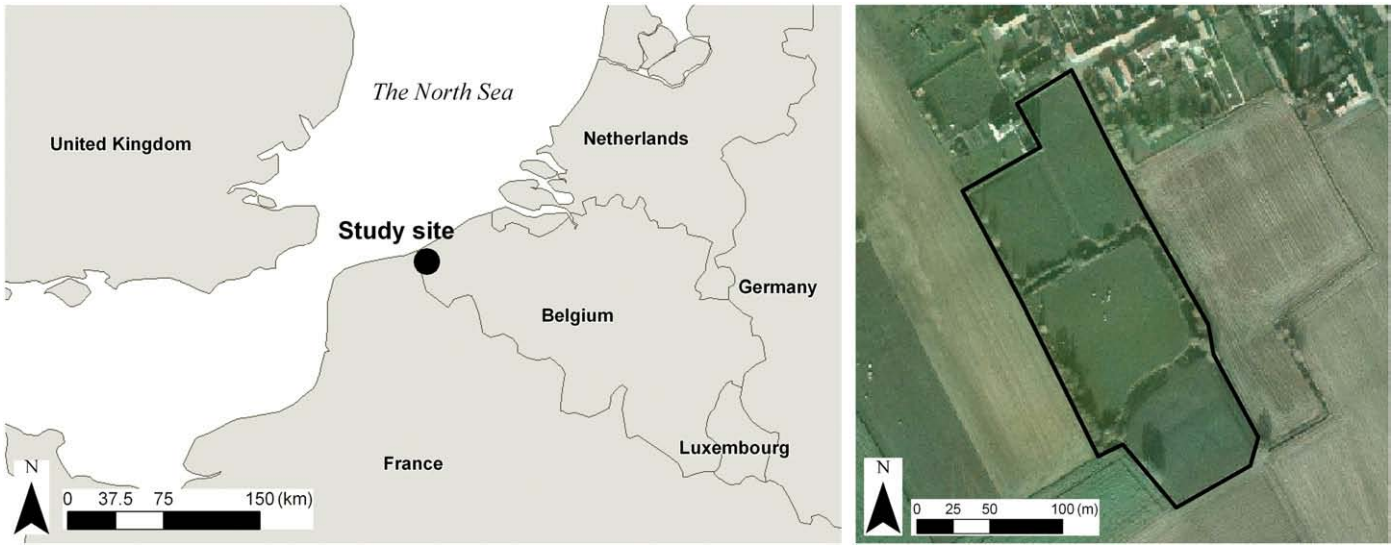

Fig. 1. Location and aerial photograph of the study site, with the delineation of the three pasture fields.

Author's personal copy

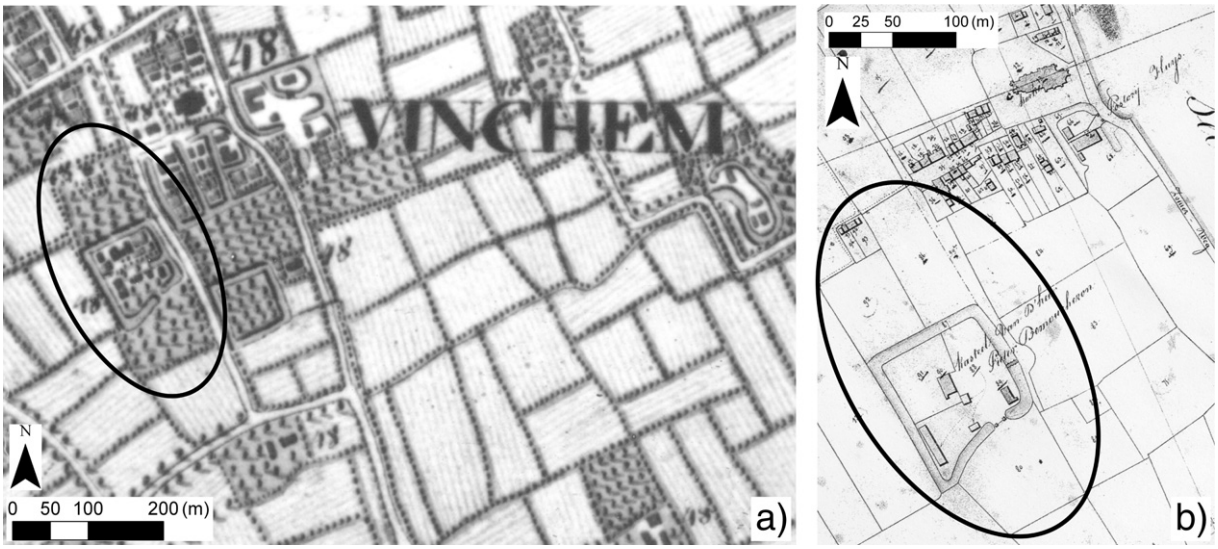

Fig. 2. a) Map of count de Ferraris (1771–1778), showing the moated site with contemporary buildings at the village of Vinkem (obtained from the Royal Library, Brussels). b) Dutch cadastral map (1818–1830), showing the castle of "de Moucheron" within the parcel, divided into different cadastral units (obtained from the Cadastral Archives, Bruges).

with the primary field) is proportional to the ECa of the soil. The in-phase (IP) response is influenced by soil constituents with a high magnetic susceptibility, hence it is proportional to the soil MSa. To summarize, the EM38DD can measure four configurations: QP in vertical coplanar (ECa-VCP) or horizontal coplanar (ECa-HCP), related to the ECa; and IP in VCP (MSa-VCP) or HCP (MSa-HCP), related to the MSa of the soil. The ECa was expressed in milliSiemens/meter (mS/m), while the MSa was expressed in dimensionless volume magnetic susceptibility units (msu) using the SI convention (msu SI).

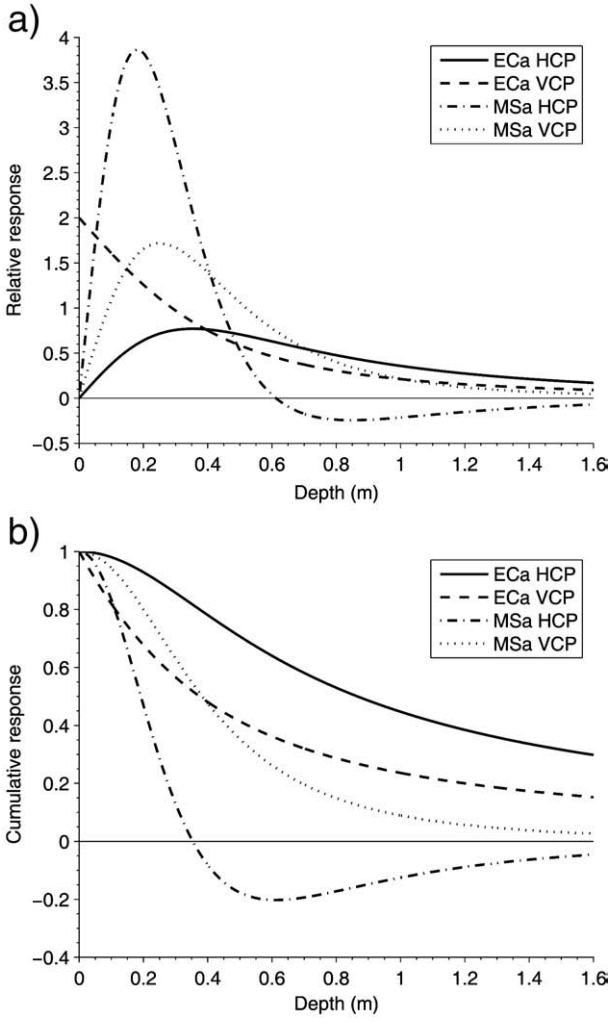

Fig. 3. Depth–sensitivity curves for the four possible EM38DD configurations.

With an intercoil distance of 1 m and a transmitter frequency of 14.6 kHz, the depth sensitivity of a layered medium under low induction number conditions (LIN) is given by McNeill (1980) and Geonics Limited (1998) and was partly based on Keller and Frischknecht (1966) (Fig. 3). These approximate solutions were matched with the exact derivations of the Maxwell formulas in the 1D layered model of Tabbagh (1986) and showed a good correspondence. Each point on the curves of Fig. 3a presents the relative response of an infinitesimally thin layer at a depth shown on the *x*-axis, while the curves on Fig. 3b are the integration of each infinitesimal layer from an infinite depth up to the depth shown on the *x*-axis. The HCP orientation receives more weight from layers below 0.4 m than the VCP for the ECa measurement. But the 3D modelling of Tabbagh (1986) showed that the HCP is theoretically less suited to detect ECa contrasts of limited lateral extent. While the VCP is entirely positive for the MSa measurement, the HCP experiences a sign change. Soil layers above 0.61 m depth contribute a positive response as the MSa-VCP, but below 0.61 m depth the response is negative. As a consequence, the cumulative weight of all layers deeper than 0.35 m is zero.

The sensor was fixed in a sled and pulled by an all-terrain-vehicle (ATV) equipped with a differential GPS (pass-to-pass accuracy 0.1 m) to georeference the sensor data (Fig. 4). The sensor was oriented parallel to the driving direction, and lay 0.05 m above the soil surface. The driving speed was 5–6 km h^{-1}, which is sufficiently slow to avoid errors due to the response time of the system. With a measurement frequency of 10 Hz, approximately every 0.14 m a point was measured in the driving line. For practical purposes, the line distance was kept at 0.85 m, which corresponds with the track distance of the ATV wheels. First, the three pasture fields were measured with the sensor in ECa-HCP and MSa-VCP mode (survey 1). Based on this survey, a square area of 50 by 50 m was selected within the central field. This area was measured with the EM38DD, in two perpendicular driving directions to survey 1, in MSa-HCP and MSa-VCP mode (survey 2). Finally, the same square area was also measured in an east–west direction with a Fluxgate gradiometer (FM256 Fluxgate Gradiometer, Geoscan, UK), operated and carried by hand (survey3). This sensor measures the vertical pseudogradient of the magnetic field strength with 0.5 m

Author's personal copy

Fig. 4. Mobile measurement configuration, showing the parallel driving lines. The sled containing the sensor was pulled in the line of the right ATV track, which was also in line with the GPS antenna. No archaeological traces were visible at the surface.

separation. Therefore, the measurement units are expressed in nT/0.5 m. The instrument resolution was 0.1 nT/0.5 m. This survey was not guided by GPS; grid lines were laid out within the square area with a tape measure with a line distance of 0.85 m. This line distance was chosen to correspond with the mobile EM38DD surveys, although denser traverse intervals are recommended for detailed archaeological surveys (English Heritage, 1995). The point distance within the lines was 0.25 m. Therefore, the EM38DD data were thinned to approach the same point distance of the gradiometer data.

2.4. Data processing

Using the EM38DD sensor on a mobile platform requires specific data processing. First, the GPS-points have to be shifted backwards within a line, to correct the spatial offset between the sensor location and the GPS antenna (a small extra shift is also caused by the data recording process). Second, the drift in time of the sensor measurements must be corrected. Therefore, just after the initial calibration, a calibration line was driven, crossing all subsequent survey lines. The difference between the calibration data and the survey data at the crossing points allowed monitoring the drift (Fig. 5). For survey 1, the maximum drift difference for the ECa-HCP was less than 0.5 mS m^{-1}, which is equal to the noise level given by Geonics Limited and low compared to the data range of survey 1. On the contrary, the maximum drift of 2.75E−4 msu SI for the MSa-VCP was considerable, compared with the data range of survey 1. Thus, the monitoring curve was used to correct the data points according to the recording time. The gradiometer data were processed with Geoplot 3.0 (Geoscan, UK). The mean of each line was set to zero, except for a few lines where the zero mean traverse treatment caused artefacts.

All the data layers were interpolated with ordinary point kriging to the same grid with a cell size of 0.2 m. Kriging has the advantage over other interpolation methods that apart from minimizing the estimation variance, it also accounts for redundancy because clustered points receive less weight than more isolated points (Goovaerts, 1997). This was important because the number of points was higher in-line than cross-line. A circular search window of 2.5 m radius was chosen, so that points of at least three driving lines were used. Finally, the maps were presented in grey scales, linearly distributed over the values but clipped at a minimum and maximum level to show the anomalies in an optimal contrast.

2.5. Soil augering

To verify the results of the geophysical survey, a total of 66 augerings were conducted along several transects, concentrated on the central field (methodology described by Simpson et al., 2008). A combination of an Edelman auger (7 cm in diameter) and a gouge auger (2 cm diameter) was used for the soil augering. The soil morphology was qualitatively described and more attention was given to artefacts and ecofacts. The maximal depth of the auger holes was between 1.5 and 2 m.

3. Results

3.1. Total site survey with EM38DD (survey 1)

The elevation of the site was obtained from a LIDAR survey, conducted for the whole Flanders with an average point density of 1 point per 20 m^2 (Fig. 6a). LIDAR or "light detection and ranging" measures the distance between an airplane and the ground by recording the travel time of a laser pulse. In general, the elevation increased gently from north to south. The ditch surrounding the central and southern field was clearly visible as a local minimum. The northern and central field had a similar elevation, while the southern field was up to 1 m higher. The field in the north was very homogeneous in both the ECa-HCP (Fig. 6b) and MSa-VCP (Fig. 6c) maps. It was divided by a north–south oriented ditch of approximately 1 m deep, where no measurements could be taken due to wetness. Only a very local extreme appeared in both configurations, probably caused by a metal object.

The central field showed strong anomalies in both maps, indicating human disturbances. The MSa-VCP map (Fig. 6c) clearly indicated the buried remains of a square brick structure. Soil augerings confirmed the presence of large concentrations of brick rubble, ceramics and walls, which were the remains of the 17th century castle located at the highest point in the central field. The square anomaly was surrounded by other anomalies, associated with smaller building remains. The

Author's personal copy

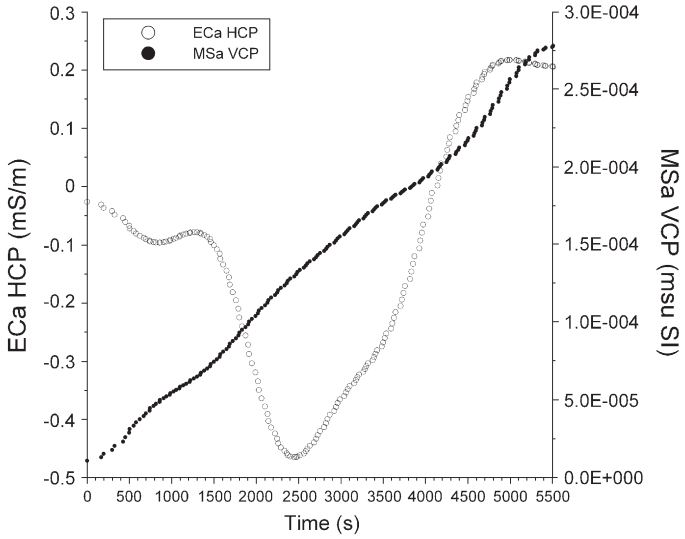

Fig. 5. Drift of EM38DD values of survey 1, for the ECa-HCP and MSa-VCP configurations.

ECa-HCP map (Fig. 6b) showed completely different anomalies than the MSa-VCP map. Around the strong magnetic anomaly, a band of higher electrical conductivity occurred. At the east side of the magnetic anomaly, a clear ditch structure with organic layers was augered. At the north and west side of the high ECa area, a shallow organic layer with a clay accumulation was found at around 0.6 m below the plough layer. So this band of high ECa probably indicated a former ditch system around the main building area.

The values of the ECa-HCP map were lower in the southern field than in the other fields. This was explained by the depth of a clay rich, Tertiary layer below the loam. Because the elevation was 1 m higher, the clay layer was deeper than in the other fields, where it was augered at 1.1 m under the soil surface. This also explained the correspondence between the local depressions in the southern field and a higher ECa, because there the clay layer was closer to the soil surface. These depressions indicated the presence of a filled-up ditch (east–west) and a rectangular area (to the west). The MSa-VCP map only showed some small disturbances close to the central field.

3.2. Comparison between EM38DD configurations and gradiometer (surveys 2 and 3)

The results of surveys 2 and 3 were used to evaluate the different EM38DD configurations together with the gradiometer measurements. In Fig. 7a and b, where the MSa-VCP configuration was measured in two perpendicular surveys, the effect of the driving direction was visible as a

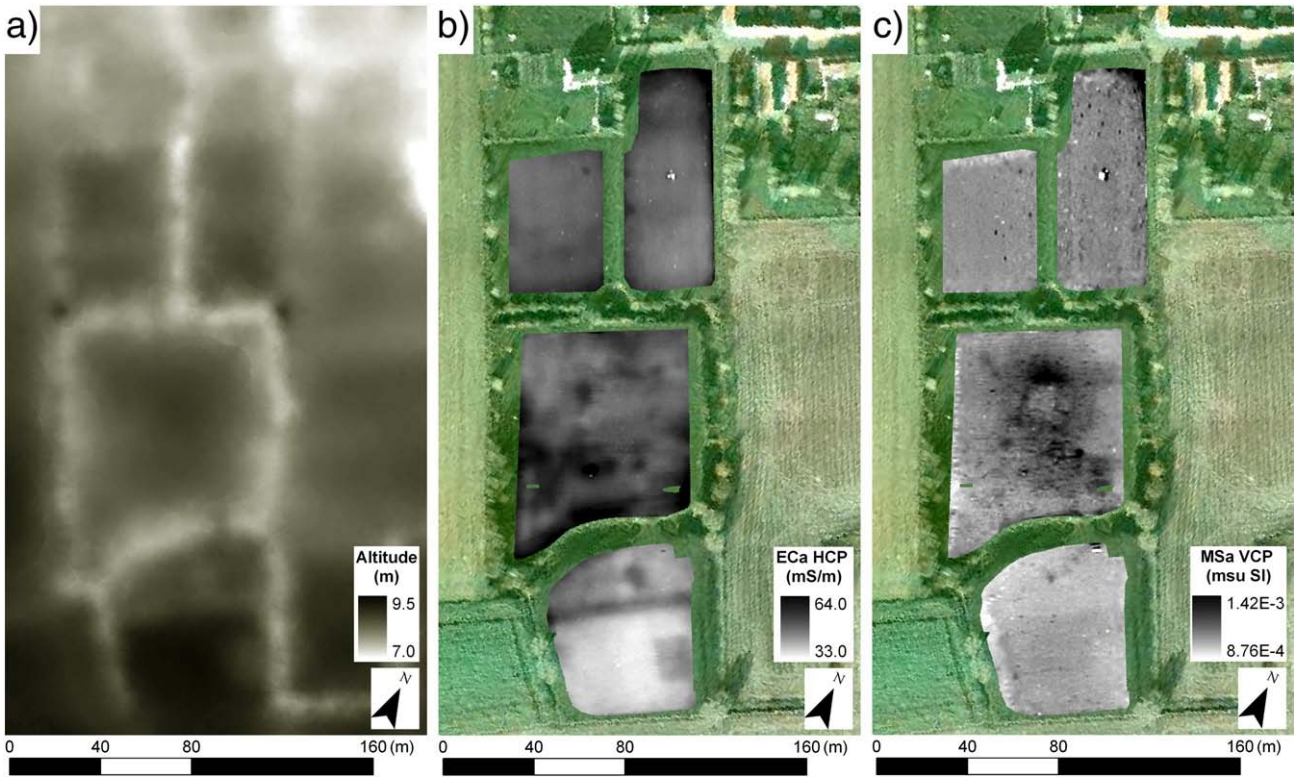

Fig. 6. a) Altitude above mean sea level (obtained from the Ministry of the Flanders Community and the Supporting Center OC-GIS Flanders), the square delineates the selected area of surveys 2 and 3; b) EM38DD MSa-VCP configuration map of the three pasture fields, with the aerial photograph as background; c) EM38DD ECa-HCP configuration map.

Author's personal copy

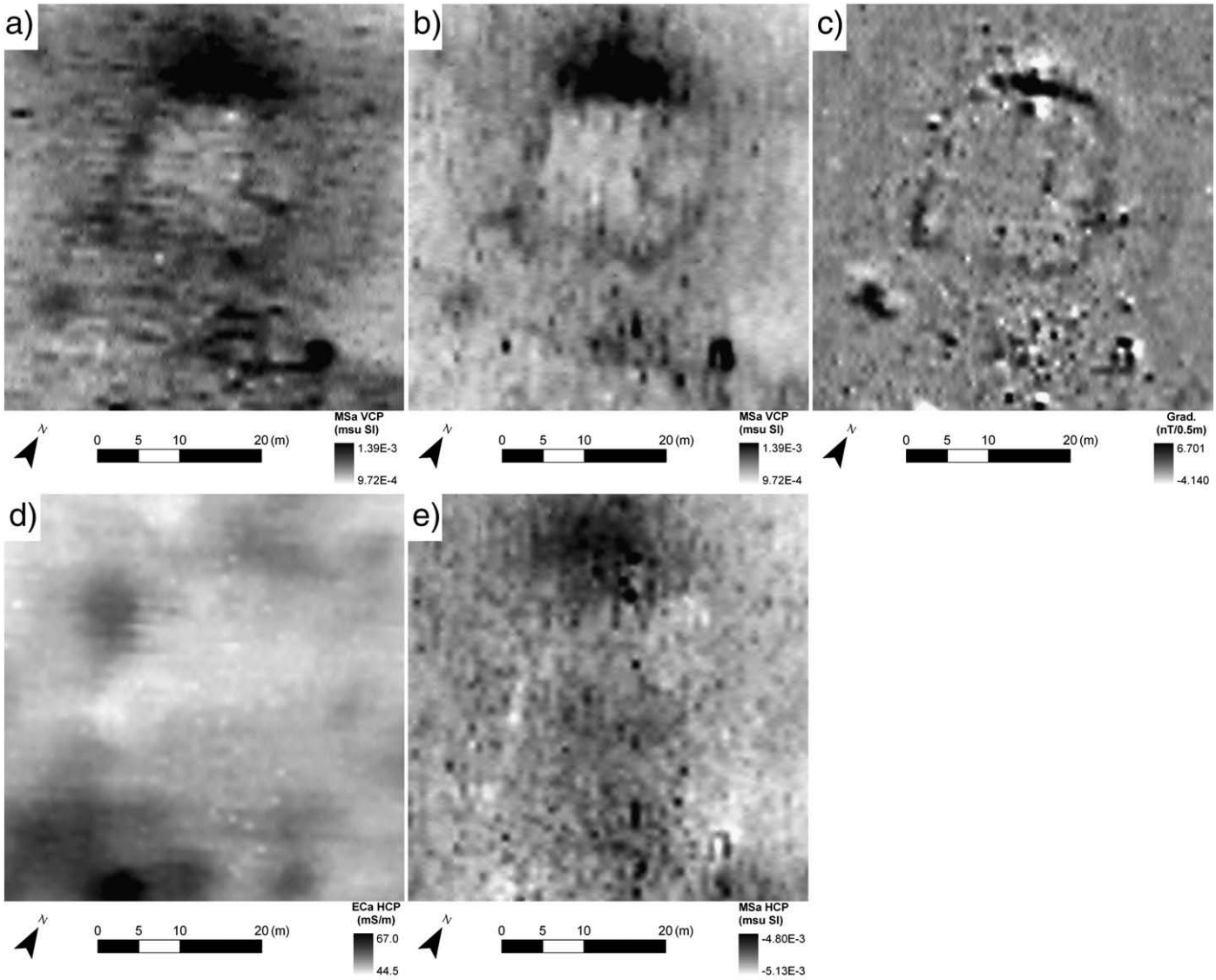

Fig. 7. EM38DD maps of survey 1, cut out to the selected square area: a) MSa-VCP and d) ECa-HCP; survey 2 with perpendicular driving direction to survey 1: b) MSa-VCP and e) MSa-HCP; survey 3: c) gradiometer map.

smearing out of the values in the driving direction. This was caused by the different sensitivity of objects parallel or perpendicular to the sensor in the horizontal plane and the response time of the system. These patterns can create anomalies that can be mistaken for actual soil anomalies. But in general the anomalies of both maps were similar. Also the maps showed a remarkable resemblance to the gradiometer map (Fig. 7c). These anomalies clearly delineated the remains of the castle and related features. Some faint anomalies could probably be attributed to internal divisions. The gradiometer anomalies had a positive peak, sometimes with a clear negative trough to the north, as can be expected in the northern hemisphere for anomalies created by induced magnetism. At Vinkem, this corresponded clearly with relatively higher values in the EM38DD MSa-VCP. The anomalies of the MSa-HCP (Fig. 7e) were far less straightforward. Both positive and negative anomalies were visible on the map. This was explained by the sign change of the relative response at 0.61 m depth (Fig. 3a), where high MS features close to the surface produce a positive response (as the MSa-HCP) and deeper features produce a negative response. In general, the MSa-HCP corresponded less with the gradiometer map than the MSa-VCP. The ECa-HCP data (Fig. 7d) showed totally different anomalies than observed by the MSa measurements, which confirmed that both phases often contain different information about the soil physical properties. It was remarkable that the brick wall remains didn't produce any anomaly on the ECa-HCP map.

Most of the magnetic anomalies were related with the presence of bricks, as found by the augerings. Large concentration of ceramics, charcoal, phosphates and both yellow and red bricks were present at the very strong anomaly in the north. At 0.65 m depth, a solid yellow brick structure was found, impossible to penetrate with the auger. Also the east and west sides of the anomaly were characterized by solid yellow brick at 0.35 m depth. At the south side, no solid structure was found, but large fragments of bricks indicated the former presence of a brick structure. At this location, the magnetic anomalies were weaker. In the southeast corner of Fig. 7, a bright red brick wall was augered at the location of the very strong magnetic response. These were the remains of a separate building associated with the main site, but which could have been constructed in another period. Brick has a certain magnetic susceptibility so that it acquires induced magnetisation (Jordanova et al., 2001), but the firing may also have caused thermoremanence. The resemblance between the gradiometer data and the MSa-VCP of the EM38DD, which is insensitive to remanent magnetisation, was an indication of the relative importance of the induced magnetisation in the bricks. Although the remanent magnetisation of brick can be up to 10 times its induced magnetisation (for 17th century bricks the

Author's personal copy

Königsberger ratio is normally clearly above 1), a random orientation of the bricks can reduce the remanent magnetisation so that it equals the induced magnetisation (Bevan, 1994).

Because all measurements were obtained at the same resolution, the maps could be evaluated on spatial detail. The fluxgate gradiometer anomaly is asymmetric and has a positive peak that is slightly shifted towards the south with respect to the feature causing the anomaly, because of the inclination of the earth's magnetic field. The magnetic susceptibility anomaly of the EM38DD is more centred above the feature. In the present example the direct comparison of raw data is significant although the difference in anomaly location could be corrected by proper processing such as reduction-to-the pole (e.g. Tassis et al., 2008) or by transforming the EMI data (Benech et al., 2002). On the other hand, the gradiometer map was clearly sharper than the EM38DD maps; the anomaly borders were more abrupt. This was partly caused by the mobile operation of the EM38DD, which smeared out the data in the driving direction. Therefore, it is vital in EMI surveys for archaeological prospection to keep the driving speed low.

4. Conclusions

The mobile EM38DD unit was able to detect the remains of the 17th century castle in the pasture fields of Vinkem. The wall foundations were clearly visible as a strong anomaly in the in-phase response of the 1 m vertical coplanar orientation, which was due to the enhanced magnetic susceptibility of the bricks. In the horizontal coplanar orientation, the anomalies were less clear and showed both positive and negative responses, which was probably caused by the change in sign of the response at a certain depth. A remarkable fact was that the quadrature-phase response, that is proportional to the ECa, didn't show the walls in horizontal coplanar orientation. This could be due to either a too low electrical contrast of the brick remains with the soil, the low sensitivity of EMI sensors to high resistive contrasts or due to the spatial sensitivity of the HCP configuration that could be less optimal for the disturbance at this depth (Tabbagh, 1990). To test these hypotheses, measurements with other coil configurations and with electrical resistivity arrays should be conducted, but this was beyond the scope of this study.

The magnetic gradiometer measurements were closely related with the in-phase response in horizontal coplanar orientation, showing also the magnetic contrast of the bricks. The anomalies were more sharply delineated, but were also more ambiguous due to the typical bipolar response. The EMI maps were slightly smeared out in the driving direction, but apart from that the maps in perpendicular driving direction were very similar.

Overall, we concluded that in this case-study the MSa measurement of the EMI sensor was successful to detect the castle remains and the ECa measurement showed other soil disturbances related to the castle. The (in)sensitivity of the ECa to the wall remains needs to be investigated further with different coil configurations.

Acknowledgements

The authors wish to thank the reviewers for their comments that greatly improved this article and the Fund for Scientific Research-Flanders (FWO), for the financial support to the research projects G.0162.06 and G.0078.06. This study was conducted in cooperation with the Flemish Land Management Institute (VLM).

References

Bevan, B.W., 1994. The magnetic anomaly of a brick foundation. Archaeological Prospection 1, 93–104.
Benech, C., Tabbagh, A., Desvignes, G., 2002. Joint inversion of EM and magnetic data for near-surface feature studies. Geophysics 67, 1729–1739.
Cockx, L., Van Meirvenne, M., De Vos, B., 2007. Using the EM38DD soil sensor to delineate clay lenses in a sandy forest soil. Soil Science Society of America Journal 71, 1314–1322.
Desvignes, G., Tabbagh, A., 1995. Simultaneous interpretation of magnetic and electromagnetic prospecting for characterization of magnetic features. Archaeological Prospection 2, 129–139.
English Heritage, 1995. Geophysical Survey in Archaeological Field Evaluation. English Heritage, UK.
Fröhlich, B., Gugler, A.I.M., Gex, P., 1996. Electromagnetic survey of a Celtic tumulus. Journal of Applied Geophysics 35, 15–25.
Gaffney, C., Gater, J., 2003. Revealing the Buried Past—Geophysics for Archaeologists. Tempus, Stroud.
Geonics Limited, 1998. Application of "dipole–dipole"electromagnetic systems for geological depth sounding. Geonics Ltd Technical Note TN-31, Ontario (Canada).
Goovaerts, P., 1997. Geostatistics for Natural Resources Evaluation. Oxford University Press, Oxford.
Jordanova, N., Petrovsky, E., Kovacheva, M., Jordanova, D., 2001. Factors determining magnetic enhancement of burnt clay from archaeological sites. Journal of Archaeological Science 28, 1137–1148.
Keller, G.V., Frischknecht, F.C., 1966. Electrical Methods in Geophysical Prospecting. Pergamon Press, New York.
Lambrecht, T., 2002. Een grote hoeve in een klein dorp: relaties van arbeid en pacht op het Vlaamse platteland tijdens de 18de eeuw. Belgisch Centrum voor Landelijke Geschiedenis 122 Gent.
Lehouck, A., Simpson, D., Vermeersch, H., Van Meirvenne, M. 2007. Geoarcheologisch onderzoek naar (post)middeleeuwse nederzettingstructuren in de ruilverkaveling Sint-Rijkers. Locatie Vinkem: Kasteel 'de Moucheron'. UGent Archeologisch Rapporten 7, Gent.
Linford, N.T., 1998. Geophysical survey at Boden Vean, Cornwall, including an assessment of the microgravity technique for the location of suspected archaeological void features. Archaeometry 40, 187–216.
McNeill, J.D., 1980. Electromagnetic terrain conductivity measurement at low induction numbers. Geonics Ltd Technical Note TN-6, Ontario (Canada).
Maillol, J.M., Ciobotaru, D.L., Moravetz, I., 2004. Electrical and magnetic response of archaeological features at the early Neolithic site of Movila lui Deciov, Western Romania. Archaeological Prospection 11, 213–226.
Persson, K., Olofsson, B., 2004. Inside a mound: applied geophysics in archaeological prospecting at the Kings' Mounds, Gamla Uppsala, Sweden. Journal of Archaeological Science 31, 551–562.
Simpson, D., Lehouck, A., Van Meirvenne, M., Bourgeois, J., Thoen, E., Vervloet, J., 2008. Geoarchaeological prospection of a medieval manor in the Dutch Polders using an electromagnetic induction sensor in combination with soil augerings. Geoarchaeology 23, 1–14.
Tabbagh, A., 1984. On the comparison between magnetic and electromagnetic prospection methods for magnetic feature detection. Archaeometry 20, 171–182.
Tabbagh, A., 1986. What is the best coil orientation in the slingram electromagnetic prospecting method? Archaeometry 28, 185–196.
Tabbagh, A., 1990. Electromagnetic prospecting. In: Scollar, I., Tabbagh, A., Hesse, A., Herzog, I. (Eds.), Archaeological Prospecting and Remote Sensing. Cambridge University Press, Cambridge, pp. 520–590.
Tassis, G.A., Hansen, R.O., Tsokas, G.N., Papazachos, C.B., Tsourlos, P.I., 2008. Two-dimensional inverse filtering for the rectification of the magnetic gradiometry signal. Near Surface Geophysics 6, 113–122.
T'Jonck, G., Moormann, F.R., 1962. Verklarende tekst bij het kaartblad Veurne 50E. Bodemkaart van België, IWONL, Gent (Belgium).